A Practical Thermodynamic Method to Calculate the Best Glass-forming Composition for Bulk Metallic Glasses

H. Wang*[a], H. M. Fu[b,c], H. F. Zhang[b], Z. Q. Hu[b]

a. Faculty of Engineering and Surveying, The University of Southern Queensland, Toowoomba, QLD 4350, Australia. E-mail: wangh@usq.edu.au

b. Shenyang National Laboratory for Materials Science, Institute of Metal Research, Chinese Academy of Sciences, Shenyang 110016, China

c. School of Engineering, The University of Queensland, St Lucia, QLD 4072, Australia

Abstract

Bulk metallic glasses (BMGs) are regarded as a new class of engineering materials because of their extraordinary high strength, great elasticity, and high corrosion and wear resistance. The selection of good glass-forming composition is the most important issue in BMG development. In this paper, a thermodynamic method, which combines element substitution and mixing enthalpy calculation, has been successfully developed to predict the optimum glass-forming compositions in Cu-Zr-Ti, Cu-Hf-Ti, Cu-Zr-Hf-Ti and Pd-Ni-P alloy systems. The prediction results prediction were confirmed by the experiments. Alloy compositions with the largest glass-forming ability (GFA) are always accompanied with the smallest enthalpy value for the alloy systems. It is concluded that the thermodynamic method provides a practical and effective tool to find the optimum glass forming composition.

Keywords: bulk metallic glasses, glass-forming ability, Miedema's model, mixing enthalpy

---

* Corresponding author

1. Introduction

Amorphous alloys or metallic glasses have attracted considerable attention due to their unique properties in mechanical, magnetic, electronic, chemical, optical and other applications. To solidify a melt into an amorphous structure, usually very high cooling rates are required [1,2]. Initially an amorphous structure was produced using the melt spinning method, in which molten metal was poured onto a spinning casting wheel, producing metallic glass ribbon [3]. The requirement for high cooling rate means that metallic glasses can only be produced in very thin shapes, which precludes these materials for any structural applications. In the late 1980’s, Inoue et al. in Tohoku University discovered that some multi-component alloys exhibited exceptional high glass-forming ability (GFA) [4,5]. The discovery means that metallic glasses can be produced in bulk shapes using conventional casting methods in these alloy systems. To develop an alloy with high GFA, multiple elements, sometimes four or five elements, are used to form a complex system. The complexity of the alloy system increases the difficulty of atomic rearrangement for crystallization, therefore suppressing nucleation and gain growth of any crystalline phase. Based on the extensive experimental data, Inoue proposed three empirical rules for the achievement of high GFA: (1) multi-component alloy systems consisting of more than three elements; (2) significant difference in atomic size ratios, above 12%, among the three main constituent elements; and (3) negative heats of mixing among the three main constituent elements. These rules have successfully acted as a guiding principle for the search of new glass-forming composition, and a great number of new bulk metallic glasses (BMGs) have been identified.

In practice, it is still difficulty to navigate in multi-component composition space to locate the best glass-forming composition. Hundreds of trial-and-error runs are required to cover the entire ternary or quaternary composition space. In this paper, based on the three empirical rules, we developed a practical method to predict the best glass-forming composition for BMGs using element substitution with thermodynamic calculation. The method has been applied successfully in Cu-Zr(Hf) and Ni-P systems, where the best glass-forming compositions are identified.

2. Thermodynamic model

The principle of the method can be described as follows: (1) start from some of the well investigated high glass-forming binary alloy systems; (2) use the element that is in the same period or group in the period table to partially substitute the existing constituent element. (3) use thermodynamic model to calculate the mixing enthalpy in the new system, and hence determine the best substitution level. Because the substitution element used has the similar atomic size and property nature, we expect that such a substitution will increase the number of the element components without the increase of mismatch entropy, which will satisfy the first and second terms of the empirical rules. The calculation of the mixing enthalpy corresponds to the third term of the rules. The best GFA comes from the composition with the lowest negative heats of mixing.

For a ternary system A-B-C or a quaternary system A-B-C-D, the mixing heat is the sum of the mixing enthalpy of the binary solid solutions in the system, which is calculated using Miedema's model [6]. Therefore,

$$\Delta H_{ABC} = \Delta H_{AB} + \Delta H_{AC} + \Delta H_{BC} \quad (1)$$

and

$$\Delta H_{ABCD} = \Delta H_{AB} + \Delta H_{AC} + \Delta H_{AD} + \Delta H_{BC} + \Delta H_{BD} + \Delta H_{CD} \quad (2)$$

respectively. ΔH is the mixing enthalpy of binary solid solution, which results from the changes in electron concentration and electronegativity when the two elements form a solid solution. Using Miedema's model, ΔH can be obtained:

$$\Delta H = f(x_A, V)g(x_A, n_{WS})p[q/p(\Delta n_{WS}^{1/3})^2 - p(\Delta\phi)^2 - a(r/p)] \tag{3}$$

where x_A , n_{WS} , Δn_{WS} and $\Delta\phi$ are the bulk concentration of element A, the density of electrons, the changes of electrons density and the changes of electronegativity, respectively. $f(x_A, V)$ is a function dependent on x_A and volume V , and $g(x_A, n_{ws})$ on x_A and n_{ws} . p and q are empirical constants. Term r is justified heuristically as the hybridization or interaction energy between the electrons of elements. The value of a is 0.73 for liquid alloys and 1 for solid.

When element A is combined with element B to form a binary solid solution or an alloy, the energy effects upon alloying are assumed to be generated at the contact surface between dissimilar cells, therefore, the surface concentrations x_A^s and x_B^s are more relevant than the bulk concentrations x_A and x_B . x_A^s can be defined by

$$x_A^s = \frac{x_A V_{Aa}^{2/3}}{x_A V_{Aa}^{2/3} + x_B V_{Ba}^{2/3}} \tag{4}$$

where V_A and V_B are the molar volumes of the pure elements. V_{Aa} and V_{Ba} are the molar volumes of the alloy elements. $x_B^s = 1 - x_A^s$. So the assumption that $f(x_A, V)$ follows the zeroth approximation to the regular solutions is adapted. With x_A^s substituted for x_A :

$$f(x_A, V) \equiv f(x_A^s, x_B^s) = x_A^s x_B^s \tag{5}$$

The surface concentration x_A^s should be expressed in terms of the volumes in the alloy V_{Aa} instead of V_A . The crude empirical relation yielding $V_{Aa}^{2/3}$:

$$V_{Aa}^{2/3} = V_A^{2/3}[1 + \mu_A x_B(\phi_A\text{-}\phi_B)] \tag{6}$$

Where μ_A is a constant. ϕ_A and ϕ_B are the electronegativity of the pure elements A and B.

The function $g(x_A, n_{WS})$ can be expressed as:

$$g(x_A, n_{WS}) = \frac{2x_A V_{Aa}^{2/3} + 2x_B V_{Ba}^{2/3}}{(n_{WS}^A)^{-1/3} + (n_{WS}^B)^{-1/3}} \tag{7}$$

Substitution of equation (3)-(7) into equation (2) yields:

$$\Delta H = f_{AB} \frac{x_A[1+\mu_A x_B(\phi_A - \phi_B)]x_B[1+\mu_B x_A(\phi_B - \phi_A)]}{x_A V_A^{2/3}[1+\mu_A(\phi_A - \phi_B)] + x_B V_B^{2/3}[1+\mu_B(\phi_B - \phi_A)]} \tag{8}$$

$$\text{where:}\ f_{AB} = \frac{2V_A^{2/3}V_B^{2/3}[q(\Delta n_{ws}^{1/3})^2 - (\Delta\phi)^2 - a(r/p)]}{(n_{ws}^A)^{-1/3} + (n_{ws}^B)^{-1/3}}$$

The mixing enthalpy ΔH of amorphous phase is obtained by multiplying the factor of 1+5(x_A^s x_B^s)^2, which is used to account for the short range order observed in the amorphous phases.

3. Results

3.1 Cu-Zr(Hf) system

Cu-Zr and Cu-Hf systems were chosen because they are the few systems that GFA is so high that BMGs can be found even in binary alloys. We started with these two binary alloy systems and calculated the mixing enthalpy for $Cu_{100-x}Zr_x$ and $Cu_{100-x}Hf_x$ (x = 0-100). The results are shown in Fig. 1. The mixing enthalpy has a negative value and its composition dependency exhibits a “U” shape for both alloy systems with a minimum vale when x = 44. The mixing enthalpies for $Cu_{54}Zr_{44}$ and $Cu_{54}Hf_{44}$ are -37.7 and – 29.3 KJ/mol respectively. They are the compositions with the lowest mixing enthalpy in their binary systems, which can be expected for the best GFA. In experimentals, Inoue et al. reported that the best GFA compositions were $Cu_{60}Zr_{40}$ and $Cu_{55}Hf_{45}$ [7]. Others reported that $Cu_{64.5}Zr_{35.5}$ alloy had the best GFA [8]. We can say that the model predicted the composition reasonably well.

Moving to the next step, $Cu_{60}Zr(Hf)_{40}$ was chosen as the base alloy, using element Ti to partially substitute Zr and Hf to turn the binary system into a Cu-Zr(Hf)-Ti ternary system. Ti is in the same group as Zr and Hf in the periodic table, Group IVA. Ti is in Period 4, while Zr and Hf are in Period 5 and 6 respectively. The reason for using $Cu_{60}Zr(Hf)_{40}$ instead of $Cu_{54}Zr(Hf)_{44}$ is because more experimental data are available for comparison. The calculation of the mixing enthalpy for $Cu_{60}Zr_{40-x}Ti_x$ and $Cu_{60}Hf_{40-x}Ti_x$ are shown in Fig. 2. Substitution by Ti initially further reduces the mixing enthalpy. After reaching the minimum value, the mixing enthalpy is increased again. For $Cu_{60}Zr_{40-x}Ti_x$, ΔH reaches the minimum value (-39.1 KJ/mol) when x = 10, while for $Cu_{60}Hf_{40-x}Ti_x$, x = 15, the value is -32.2 KJ/mol. In experiments, Inoue et al. reported [9,10] the largest diameter BMG rods of 2 mm were formed in $Cu_{60}Zr_{30}Ti_{10}$ and $Cu_{60}Hf_{25}Ti_{15}$. The compositions were exactly what the model predicted. In the ternary system, increasing the component number from 2 to 3 further reduces the heats of mixing for the systems, therefore the GFA is increased and the critical sizes of the BMG sample are increased.

Following the same method, we now substitute Zr and Hf with each other to further increase the component number from 3 to 4, forming a quaternary system. For $Cu_{60}Zr_{30}Ti_{10}$, Zr is partially substituted by Hf, forming $Cu_{60}Zr_{30-x}Hf_xTi_{10}$. While for $Cu_{60}Hf_{25}Ti_{15}$, Hf is partially substituted by Zr, forming $Cu_{60}Hf_{25-x}Zr_{-x}Ti_{15}$. Fig. 3 shows the calculation results of the mixing enthalpy for the quaternary systems. Partial substitution of Zr and Hf, further brings down the mixing enthalpy for the alloy systems. For $Cu_{60}Zr_{30-x}Hf_xTi_{10}$, the substitution leads to the minimum heat of mixing at -41.0 KJ/mol when x = 10. The model prediction again lies exactly with the experimental results, which reported that $Cu_{60}Zr_{20}Hf_{10}Ti_{10}$ has the best GFA in Cu-Zr-Hf-Ti quaternary system [9,11]. The substitution in $Cu_{60}Hf_{25-x}Zr_{-x}Ti_{15}$ results in a minimum mixing enthalpy value when x = 6. Unfortunately, there is no experimental result available to check the GFA for this composition.

3.2 Ni-P system

Ni-P is another binary alloy system that has a large GFA. Metallic glass has been obtained in $Ni_{80}P_{20}$ alloy using melt spinning method [12]. It has been reported that GFA is significantly improved when palladium is introduced to make the binary system into a ternary system [13]. To determine the best composition for formation of BMGs, He et al. [13] experimentally investigated the whole composition range of the system. The results concluded that BMG (diameter range between 10-25 mm) can be synthesized within the composition range 25-60 at.% Pd, 20-57 at.% Ni and 16-22 at.% P. Of all the alloy compositions examined, $Ni_{40}Pd_{40}P_{20}$ had the highest glass formability with an amorphous cylinder at 25 mm in diameter. These conclusions were derived after numerous experimental trials to cover the whole composition space.

Here again, we used the thermodynamic method, calculating the heats of mixing for the system. $Ni_{80}P_{20}$ was chosen as the base alloy, and palladium was used to partially substitute nickel, forming $Ni_{80-x}Pd_xP_{20}$. Pd and Ni are in the same group (Group VIII) in the period table. The calculation of the mixing enthalpy is shown in Fig. 4. The mixing enthalpy has a negative value and exhibits a “U” shape for its composition dependency. The bottom of the mixing enthalpy is relatively flat, with a minimum value of about 270 KJ/mol when x = 33-41. The result agrees well with the experimental results from He et al., where x = 40 was identified as the best glass forming alloy. The large negative vale also indicates why a large critical size of BMG was fabricated in this alloy. It is very likely that we can use the same method to extend the ternary alloy system further into a quaternary system to achieve an even better GFA.

4. Discussion

To determine the GFA and locate the composition with a high GFA upon melt solidification, several criteria have been developed. Among them, the more commonly used are the reduced glass-transition temperature T_{rg} (= T_g/T_l, where T_g and T_l are the glass-transition temperature and liquidus temperature, respectively) and the supercooled liquid region ΔT (= T_x-T_g, where T_x is the onset crystallization temperature) [14]. These criteria seemed to work well in many amorphous alloy systems developed in the early stage. However, they cannot successfully predict the trend of GFA in many recently developed bulk amorphous systems. Lu [14] et al. combined these two parameter together and introduced a new criterion $\gamma = T_x/(T_g+T_l)$. These criteria usually do not have the desired predictive power to capture the composition dependency of GFA, and require input (temperature parameters) that has to be obtained only after the glasses are formed. Therefore we could not reduce the number of the experimental trials. Currently the most widely and practically adopted approach to improving the GFA of an alloy is the multi-component recipe, which follows Inoue's empirical rules [15]. The Inoue's rules actually contain the components of reduced glass-transition temperature and supercooled liquid region. The three terms of the rules, i.e. the number of element, atomic size difference and the heat of mixing, can be expressed by the thermodynamic functions for the multi-component systems, i.e. mismatch entropy and mixing enthalpy. If the substitution element comes from the same group in the periodic table, they have a similar atomic size and the same crystal structure, as illustrated in Table 1. The mismatch entropy due to the difference of atomic size is very small compared to the mixing enthalpy and can be ignored. Therefore we use the calculation of the mixing enthalpy to describe the GFA, which will give a direct composition dependency of GFA. Table 2 summarizes the comparison of the calculated results and the experimental results. The thermodynamic method successfully predicted the best composition for BMG formation. As we increased the number of element component, moving from binary system, ternary system, to quaternary system, the calculated mixing enthalpy led to a bigger negative value, and in experiments this also led to a larger critical size for produced

BMG. Hence in the same alloy system, the mixing enthalpy can be used to describe GFA when the mismatch entropy is constant.

The Miedema’s model is obtained by expanding the Wigner-Seitz theory for pure element, and the elements in binary alloy are thought as a hypothetical mechanical mixture of atoms [6]. For the Zr-Ti, Zr-Hf, Hf-Ti and Ni-Pd binary systems, they all form complete solid solutions, as shown in Fig. 5 [16], which means the premise of Miedema’s model has been met. From the Miedema’s model, the mixing enthalpies between different elements can be obtained. In the Cu-Zr(Hf) system, the mixing enthalpies between the main constituent elements are -28.86 kJ/mol for Cu-Zr, -22.51 kJ/mol for Cu-Hf and -17.57 kJ/mol for Cu-Ti. The mixing enthalpies between the substitution element and the element to be substituted are -0.06 kJ/mol for Zr-Ti, -0.21 kJ/mol for Zr-Hf and 0.13 kJ/mol for Ti-Hf. We can see the interactions between these elements are small. The interactions of Cu-Zr, Cu-Hf and Cu-Ti play a decisive role in the final mixing enthalpies of amorphous alloys. Similarly, in Ni-P system, the mixing enthalpies between the large and small atoms are -178.54 kJ/mol for Ni-P and -193.72 kJ/mol for Pd-P, while the mixing enthalpy between Pd and Ni is -0.05 kJ/mol. It is the interactions between the large and small atoms that controls the GFA, which has also been experimentally proven [17].

5. Conclusions

A practical method has been developed to predict the best glass-forming composition for bulk metallic glasses. The method combines element substitution, which uses the elements in the same period or group in the period table for substitution, and thermodynamic calculation of mixing enthalpy for substitution levels. Alloy compositions with the smallest enthalpy value have the best GFA. The method has been tested in Cu-Zr-Ti, Cu-Hf-Ti, Cu-Zr-Hf-Ti and Pd-Ni-P alloy systems, and the calculated composition successfully predicted the experimental results. The method provides a practical and effective tool for the development of new bulk amorphous alloys.

Acknowledgment

The authors are grateful for the financial supports of the National Natural Science Foundation of China (50471077, 50395100), the Foundation of Chinese Academy of Sciences (KGCX2-SW-214), the Ministry of Science and Technology of China (2005DFA50860) and the Australia Research Council under its International Linkage program.

References

[1] Clement, W., Willens, R.H., Duwez P. Non-crystalline structure in solidified gold-silicon alloys, *Nature*, 187 (1960), 869-870

[2] Chen, H.S., Turnbull, D. Evidence of a glass-liquid transition in a gold-germanium-silicon alloy, *The Journal of Chemical Physics*, 48 (1968), 2560-2571,

[3] Bagley, B.G., Chen, H.S., Turnbull, D. Characterization of amorphous alloy films, *Materials Research Bulletin*, 3 (1968), 159-168

[4] Inoue, A., Zhang, T., Masumoto, T. Aluminum-lanthanum-nickel amorphous alloys with a wide supercooled liquid region, *Materials Transactions, JIM*, 30 (1989), 965-972

[5] Inoue, A., Kita, K., Zhang, T., Masumoto, T. An amorphous $La_{55}Al_{25}Ni_{20}$ alloy prepared by water quenching. *Materials Transactions, JIM*, 30 (1989), 722-725

[6] Bokeen, N.A. “Statistical thermodynamics of alloys” Plenum Press, New York and London, 1986

[7] Inoue, A., Zhang, W. Formation, thermal stability and mechanical properties of Cu-Zr and Cu-Hf binary glassy alloy rods, *Materials Transactions, JIM*, 45 (2004), 584-587

[8] Wang, D., Li, Y., Sun, B.B., Sui, M.L., Lu, K., Ma, E. Bulk metallic glass formation in the binary Cu-Zr system, *Applied Physics Letters*, 84 (2004), 4029-4031

[9] Inoue, A., Zhang, W., Zhang, T., Kurosaka, K. High-strength Cu-based bulk glassy alloys in Cu-Zr-Ti and Cu-Hf-Ti ternary systems. *Acta Materialia*, 49 (2001), 2645-2652

[10] Park, E.S., Chang, H.J., Kim, D.H., Kim, W.T. Kim, Y.C., Kim, N.J, Formation of amorphous phase in melt-spun and injection-cast Cu60Zr30Ti10 alloys, *Script Materialia*, 51 (2004), 221-224

[11] Inoue, A., Zhang, W., Zhang, T., Kurosaka, K. Cu-based bulk glassy alloys with good mechanical properties in Cu-Zr-Hf-Ti system. *Materials Transactions, JIM*, 42(2001), 1805-1812

[12] Mentese, S., Suck, J.B., Dianoux, A.J. Atomic dynamics of amorphous and nanocrystalline Ni80P20, Part 1&2: Metastable, Mechanically alloyed and Nanocrystalline Materials, *Materials Science Forum*, 343-3 (2000), 671-676

[13] He, Y., Schwarz, R.B., Archuleta, J.I. Bulk glass formation in the Pd–Ni–P system, *Applied Physics Letters*, 69 (1996), 1861-1863

[14] Lu, Z.P., Liu, C.T. A new glass-forming ability criterion for bulk metallic glasses, *Acta Materialia*, 50 (2002), 3501-3512

[15] Inoue, A. High-strength bulk amorphous alloys with low critical cooling rates, *Materials Transactions, JIM*, 36 (1995), 866-875

[16] Villars, P., Prince, A., Okamoto, H. “Binary alloy phase diagrams” ASM International, NewYork, 1990

[17] Inoue, A. Stabilization of Metallic supercooled liquid and bulk amorphous alloys. *Acta Materialia.* 48 (2000), 279-306

Figure Captions

Fig.1 The mixing enthalpy ΔH dependence of the atomic percentage x in $Cu_{100-x}Zr_x$ and $Cu_{100-x}Hf_x$ binary alloys

Fig. 2 The mixing enthalpy ΔH dependence of the atomic percentage x in $Cu_{60}Zr_{40-x}Ti_x$ and $Cu_{60}Hf_{40-x}Ti_x$ ternary alloys

Fig. 3 The mixing enthalpy ΔH dependence of the atomic percentage x in $Cu_{60}Zr_{30-x}Hf_xTi_{10}$ and $Cu_{60}Hf_{25-x}Zr_{-x}Ti_{15}$ quaternary alloys

Fig.4 The mixing enthalpy ΔH dependence of the atomic percentage x in $Ni_{80-x}Pd_xP_{20}$ ternary alloys

Fig.5 The phase diagrams of (a) Zr-Ti, (b) Zr-Hf, (c) Hf-Ti, and (d) Ni-Pd binary alloys

Table.1 Atomic radius, crystal structure, and position in the period table of the elements in the studied alloy systems

Table 2. The comparison of experimental and calculated results

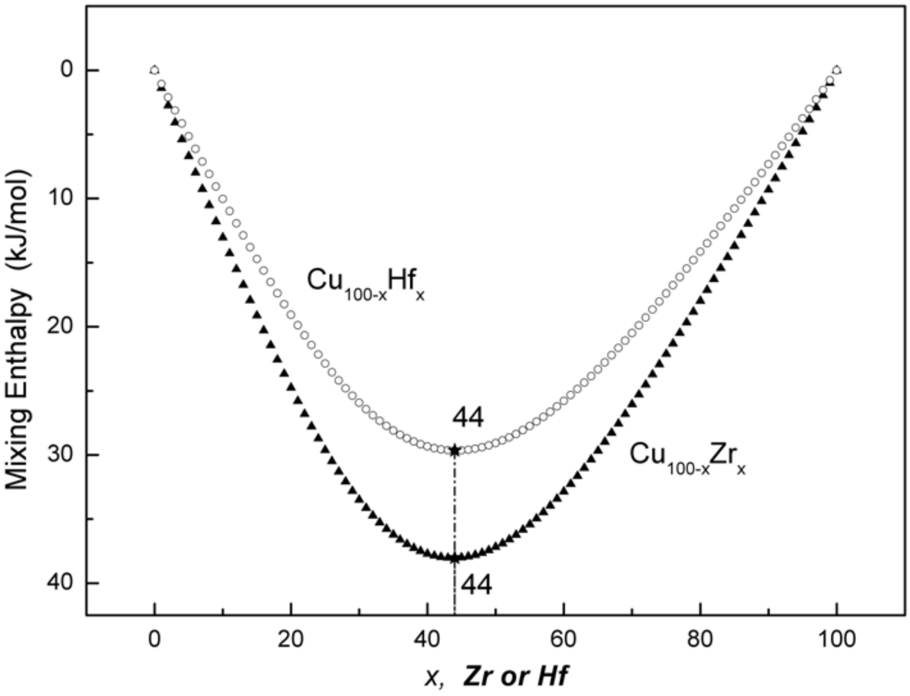

Fig.1 The mixing enthalpy ΔH dependence of the atomic percentage x in $Cu_{100-x}Zr_x$ and $Cu_{100-x}Hf_x$ binary alloys

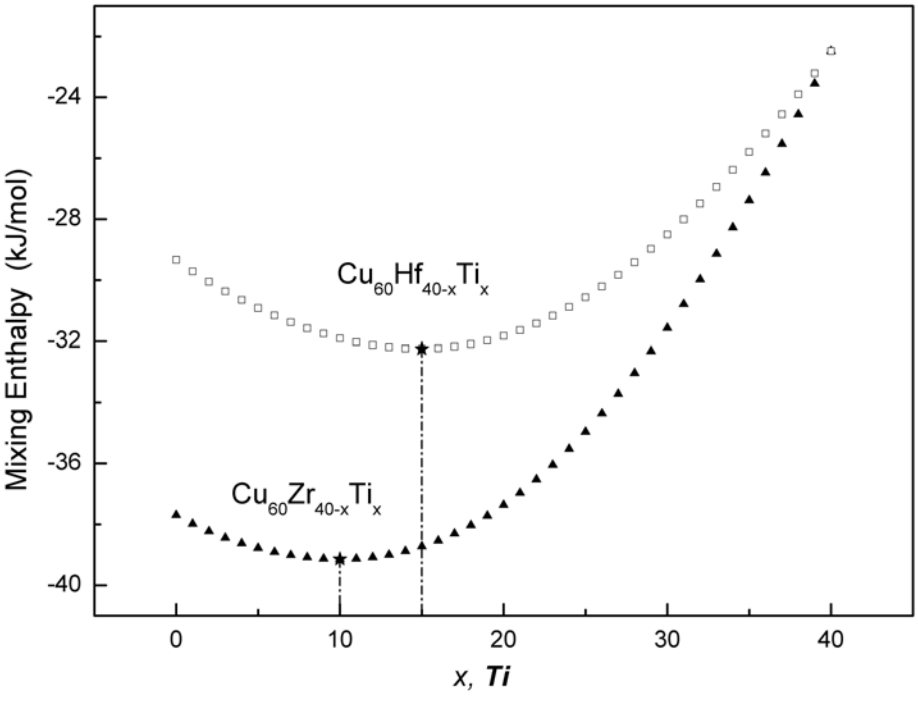

Fig. 2 The mixing enthalpy ΔH dependence of the atomic percentage x in $Cu_{60}Zr_{40-x}Ti_x$ and $Cu_{60}Hf_{40-x}Ti_x$ ternary alloys

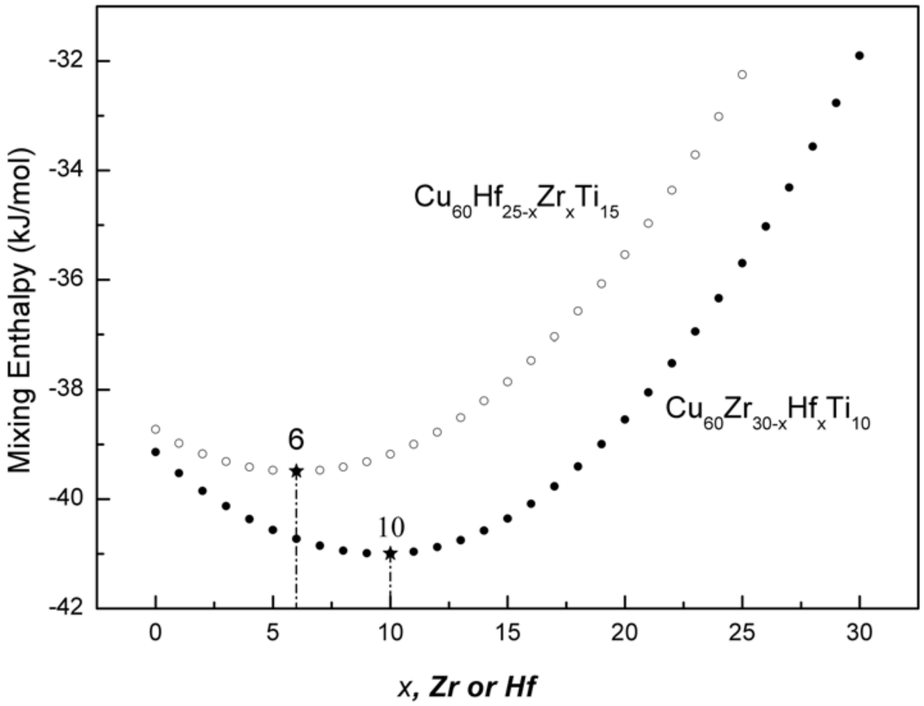

Fig. 3 The mixing enthalpy ΔH dependence of the atomic percentage x in $Cu_{60}Zr_{30\text{-}x}Hf_xTi_{10}$ and $Cu_{60}Hf_{25\text{-}x}Zr_{\text{-}x}Ti_{15}$ quaternary alloys

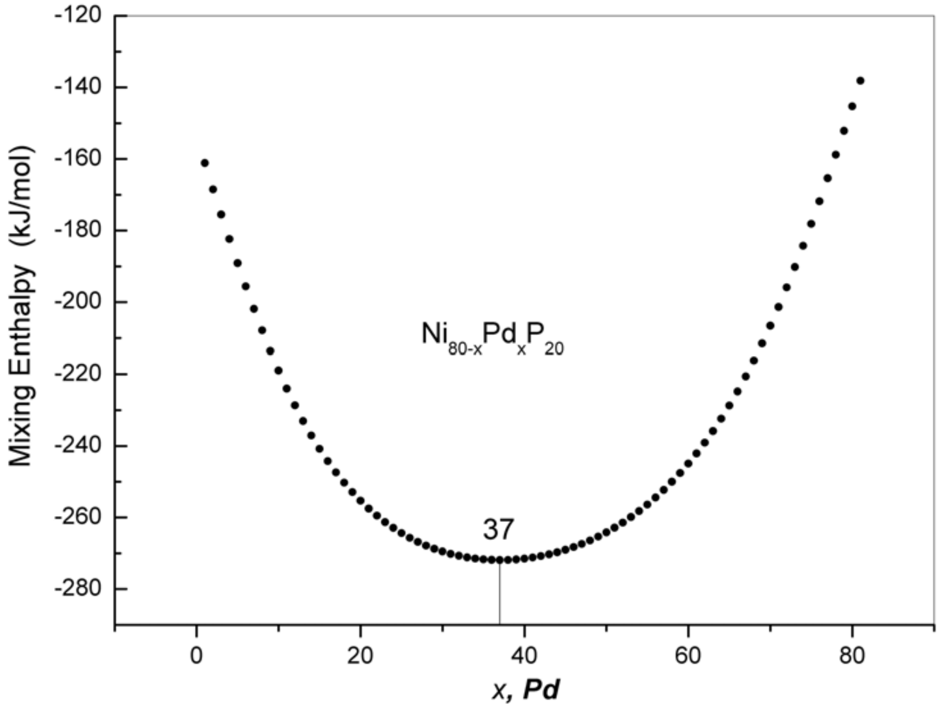

Fig.4 The mixing enthalpy ΔH dependence of the atomic percentage x in $Ni_{80\text{-}x}Pd_xP_{20}$ ternary alloys

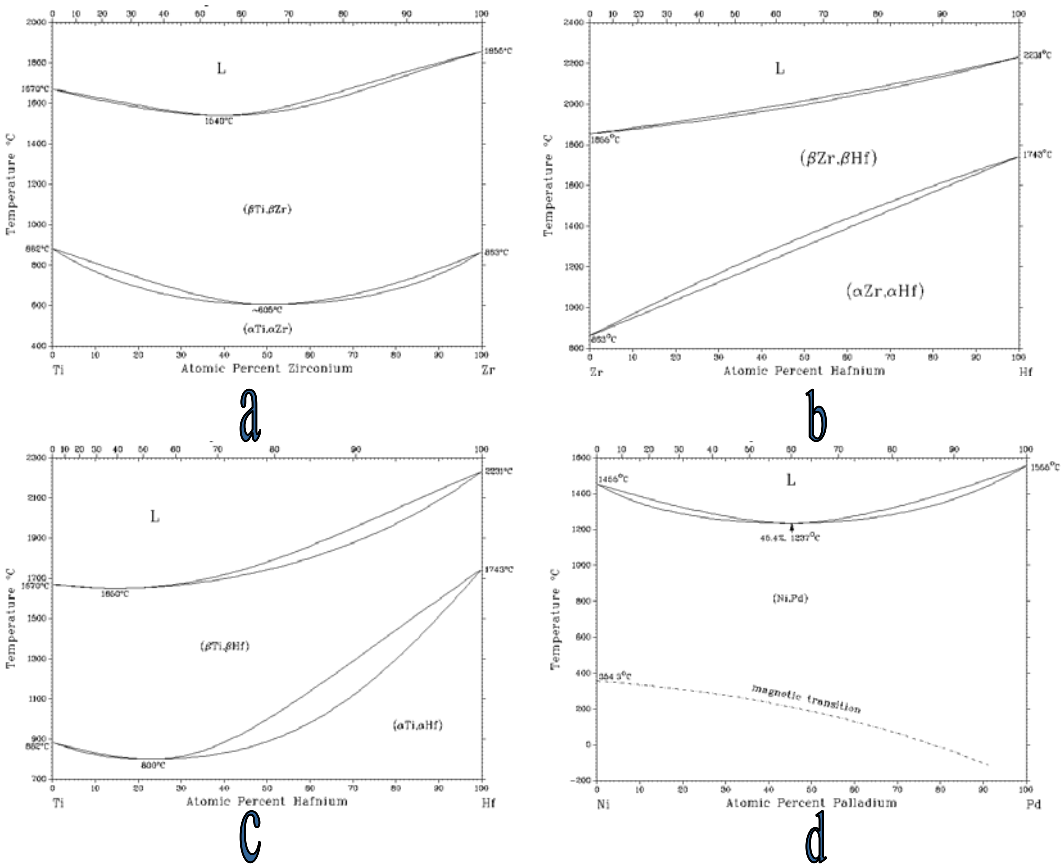

Fig. 5 the phase diagrams of (a) Zr-Ti, (b) Zr-Hf, (c) Hf-Ti and (d) Ni-Pd binary alloys

Table.1 Atomic radius, crystal structure, and position in the period table of the elements in the studied alloy systems

Element	**Zr**	**Hf**	**Ti**	**Ni**	**Pd**
Atomic radius(Å)	2.16	2.16	2.00	1.62	1.79
Crystal structure	Hexagonal	Hexagonal	Hexagonal	fcc	fcc
Group	IVA	IVA	IVA	VIIIA	VIII
Period	5	6	4	4	5

Table 2. The comparison of experimental and calculated results

Alloy system	**Best composition from calculation**	**ΔH (KJ/mol)**	**Best composition from experiment**	**BMG critical size from experiment**
Cu-Zr binary	$Cu_{56}Zr_{44}$	-37.7	$Cu_{60}Zr_{40}$ [7] $Cu_{64.5}Zr_{35.5}$ [8]	>1 mm
Cu-Zr-Ti ternary	$Cu_{60}Zr_{30}Ti_{10}$	-39.1	$Cu_{60}Zr_{30}Ti_{10}$ [9]	2 mm
Cu-Zr-Hf-Ti quaternary	$Cu_{60}Zr_{20}Hf_{10}Ti_{10}$	-41.0	$Cu_{60}Zr_{20}Hf_{10}Ti_{10}$[11]	4 mm
Cu-Hf binary	$Cu_{56}Hf_{44}$	-29.3	$Cu_{55}Hf_{45}$ [7]	Ribbon
Cu-Hf-Ti ternary	$Cu_{60}Hf_{25}Ti_{15}$	-32.2	$Cu_{60}Hf_{25}Ti_{15}$ [9]	2 mm
Cu-Hf-Zr-Ti quaternary	$Cu_{60}Zr_{19}Hf_{6}Ti_{15}$	-39	------	----